Original Article

Experimental Measurement of Magnetization of a Rectangular Bar-shaped Permanent Magnet Utilizing MFMIM

M. Kabir[1], H. R. Mashayekhi[2], S. Aftabi[3], H. Khodajou-Chokami[4*]

1- Amirkabir University of Technology (Tehran Polytechnic), Energy Engineering and Physics Department, Tehran, Iran.

2- Shahid Bahonar University of Kerman, Faculty of Physics, Kerman, Iran.

3- University of Manitoba, Department of physics and astronomy, Winnipeg, Canada.

4- Sharif University of Technology, Energy Engineering Department, Tehran, Iran.

Received: 9 February 2016
Accepted: 7 May 2016

Keywords:
MFMIM,
Magnetization,
Magnetic Resonance Imaging (MRI),
Experimental Measurement,
Permanent Magnet.

A B S T R A C T

Purpose- In this investigation, after designing an experimental setup, the magnetization parameter of a rectangular bar-shaped permanent magnet has been determined by a Magnetic Field Magnitude and Intensity Meter device.

Methods- In order to achieve this purpose, after finding the geometrical center of mass of the magnet, by moving Hall-Effect sensor in 5mm steps, the magnetic flux intensity has been measured by our recently patented device.

Results- The accuracy of the experimental values in comparison with the available commercial grade and analytical equations demonstrated have been confirmed. Our device's results accuracy has also been approved by benchmarking all results. Following that, the magnetization parameter has been extracted using the numerical technique.

Conclusion- Results showed very precise benchmarking and proved the use of this device in measuring the magnetic field in MRI devices. This study will be directed to simulate several subjects like calculating the induced electromotive force.

1. Introduction

The Magnetic Field Magnitude and Intensity Meter (MFMIM) device application for measuring the magnetic flux intensity (B) and magnetic field intensity (H) which is based on magnetic Hall-Effect phenomenon has been presented in this paper [1]. The importance of design and fabrication of these kinds of devices is firstly their widespread use in science and engineering. Previous apparatuses which fabricated for these kinds of goals are similar in their basic goal that is measuring the magnetic flux intensity. The first attempt to create a device for measuring magnetic field magnitude was performed in the nineteenth century by Karl Friedrich Gauss and his apparatus was called the magnetometer. In the following years a variety of methods were used to measure the magnetic field [2, 3]. With the advancement of science and technology and making many changes in manufacturing semiconductor devices, semiconductor sensors were provided in order to detect and measure the magnetic field. Magnetic sensors categories according to the size and their usage in the magnetic field sensing device are showed in Figure 1. [4].

[*]***Corresponding Author:***
Hamidreza Khodajou-Chokami, PhD Student
Room 1, 2th floor, Department of Energy Engineering, Sharif University of Technology, Tehran, Iran.
Tel: +98 937 416 6317
Email: hamidreza.khodajou@gmail.com

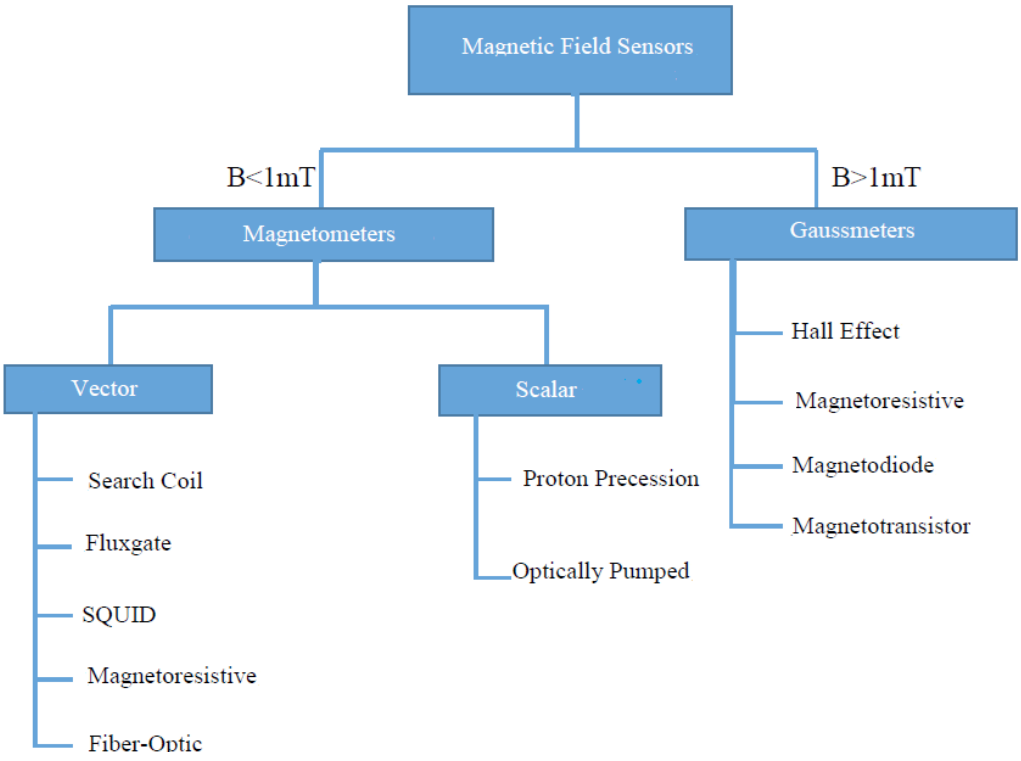

Figure 1. Types of magnetic field sensors regarding to magnitude of magnetic field.

Commercially available devices do not calculate physical parameters such as the magnitude of the magnetic field and the magnetic intensity in environments with different permeability coefficients. Disconnect the computer, limited and low speed of sample reading and the lack of manually entering the required physical parameters are other technical weaknesses of the systems that is known as Gaussmeter or Teslameter. The purpose of design and construction of the MFMIM is to fix the aforementioned flaws and simultaneously keep the unity characteristics as well as simplicity in operating. Another advantage of this system in comparison with other commercial devices is data recording frequency which varies in 1000 sample per second to 1 sample per minute and the feasibility of analysis of recorded data by statistical analysis software. Figure 2 shows the operational flowchart of MFMIM for achieving the goals mentioned above. In this study, the magnetization parameter of a bar-shaped permanent magnet has also been obtained empirically and analytically. In Figure 3 MFMIM device has been shown. In each permanent magnet [5] the magnetic dipoles' movements lead to generate a magnetic field [6]. If the magnetic moment of the ith atom is m_i, macroscopic vector quantity which is called magnetization (M) is the sum of all the dipole moments in a small volume element and it is defined as follows:

$$M = \lim_{\Delta v \to 0} \frac{1}{\Delta v} \sum_i m_i \qquad (1)$$

Where M is the magnetization parameter which is defined as a summation of all microscopic magnetic dipoles' moment (m_i) divided by a specific volume when the volume is too small. Magnetization, in fact shows the magnetic dipole moment per unit volume by the symbol of M and the units of A/m [7]. Further microscopic study of the magnetization is possible only through the quantum mechanics. This parameter is very important in physics and industry and has numerous applications in the cases such as physics accelerators [8], designing and manufacturing electric motors [9], medical magnetic resonance

imaging (MRI) [10,11], geologic [12] and superconductivity [8]. Conventional methods to obtain magnetization parameters commonly used for thin films or permanent magnets included Vibrating Sample Magnetometer (VSM), Alternating Gradient-Filed Magnetometer (AGFM) and Superconducting Quantum Interference Device (SQUID) [12].

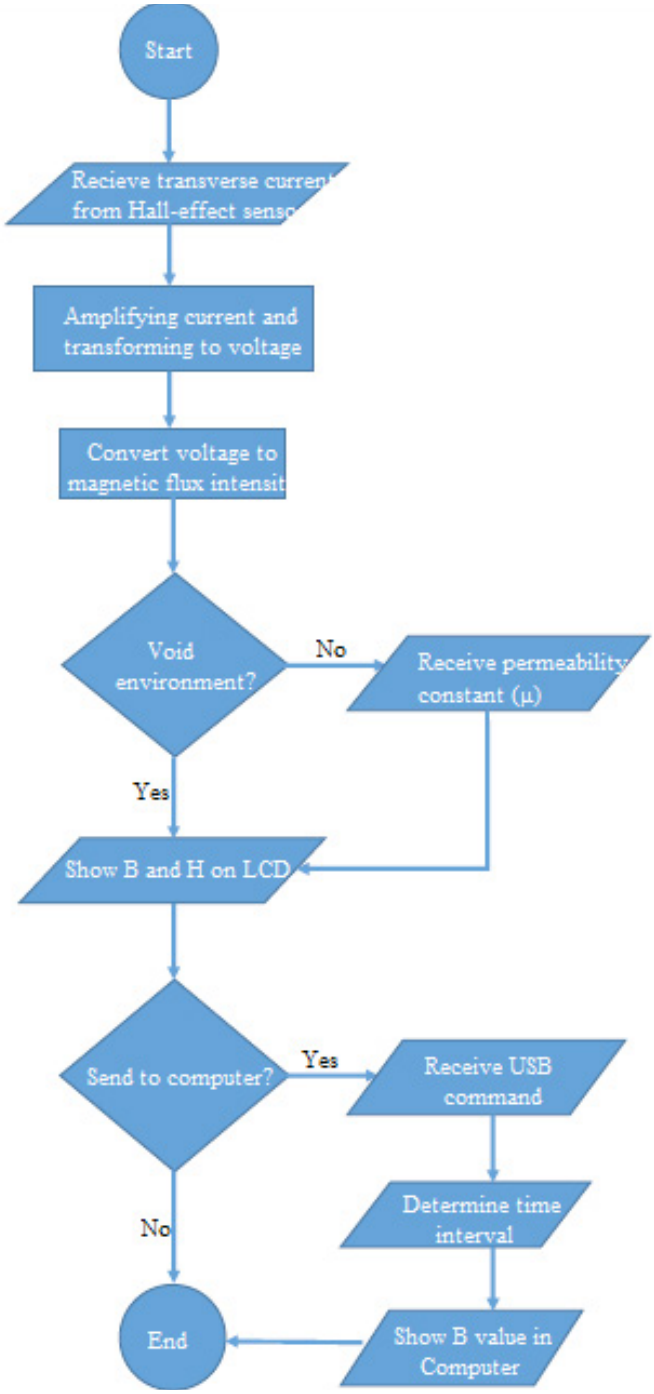

Figure 2. Operation flowchart of MFMIM.

Figure 3. MFMIM apparatus.

2. Materials and Methods

2.1. Experimental Validation

Results were obtained through MFMIM device compared with measurements with a Gauss meter model HT201 Gaussmeter fabricated in Hengtong magnetoelectricity CO [13]. The results showed very accurate benchmarking by the experimental results. Thus MFMIM output data was verified experimentally. The Hall Effect sensor which is used in MFMIM is able to measure the range of magnetic field magnitude up to 2 Tesla in steps of 3 Gauss [1]. In the following sections, an accurate performance of the device according to experimental data and theoretical benchmark is confirmed. Our exact benchmarking is shown in Figure 4.

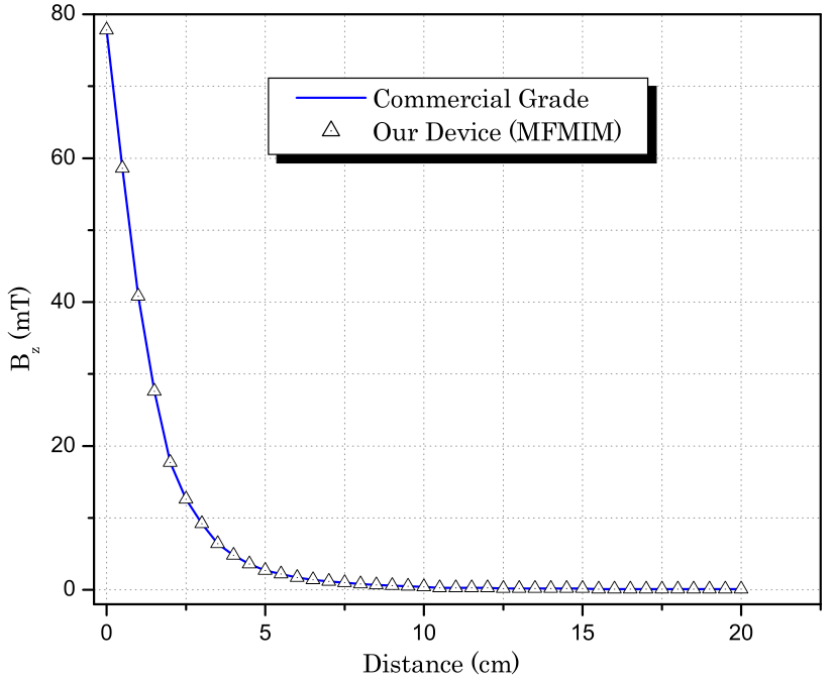

Figure 4. Benchmarking of magnetic flux intensity of MFMIM outputs and commercial grade in z-direction.

2.2 Theoretical Formulae

Assuming a constant magnetization M_0 in the positive Y-direction, the analytical expression for the stray magnetic field intensity of a bar-shaped permanent magnet has been derived in three dimensions in the x-y-z coordinate system as follows [14]:

$$H_x(x,y,z)=\frac{M_0}{4\pi}\sum_{k,l,m=1}^{2}(-1)^{k+l+m}$$
$$\ln\left\{z+(-1)^m z_b+\sqrt{\left[x+(-1)^k x_b\right]^2+\left[y+(-1)^l y_b\right]^2+\left[z+(-1)^m z_b\right]^2}\right\} \quad (2)$$

$$H_y(x,y,z)=-\frac{M_0}{4\pi}\sum_{k,l,m=1}^{2}(-1)^{k+l+m}\frac{\left[y+(-1)^l y_b\right]\left[x+(-1)^k x_b\right]}{\left|y+(-1)^l y_b\right|\left|x+(-1)^k x_b\right|}$$
$$\times\arctan\left\{\frac{\left|x+(-1)^k x_b\right|\cdot\left[z+(-1)^m z_b\right]}{\left|y+(-1)^l y_b\right|\cdot\sqrt{\left[x+(-1)^k x_b\right]^2+\left[y+(-1)^l y_b\right]^2+\left[z+(-1)^m z_b\right]^2}}\right\} \quad (3)$$

$$H_z(x,y,z)=\frac{M_0}{4\pi}\sum_{k,l,m=1}^{2}(-1)^{k+l+m}$$
$$\ln\left\{x+(-1)^k x_b+\sqrt{\left[x+(-1)^k x_b\right]^2+\left[y+(-1)^l y_b\right]^2+\left[z+(-1)^m z_b\right]^2}\right\} \quad (4)$$

Where x_b, y_b and z_b are respectively half of x, y and z dimensions' size of the bar-shaped permanent magnet. Therefore, the dimensions of the magnetized volume are $2x_b$, $2y_b$, and $2z_b$. Now if we wish to use the above formulae in a new XYZ coordinate system in which the magnetization direction is aligned in the Z-direction, then we need to rotate the xyz coordinate clockwise around x-axis by 90˚ as shown in Figure 5.

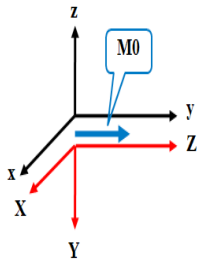

Figure 5. The two coordinate systems xyz and the XYZ. The XYZ coordinate is obtained by 90˚ clockwise rotation of xyz around x-axis.

This rotation brings Z axis in the M_0 direction. The transformation matrix to relate the magnetic H-field and the coordinate variables is given by [15]:

$$\begin{bmatrix}1 & 0 & 0\\ 0 & \cos(-90°) & \sin(-90°)\\ 0 & -\sin(-90°) & \cos(-90°)\end{bmatrix}=\begin{bmatrix}1 & 0 & 0\\ 0 & 0 & -1\\ 0 & 1 & 0\end{bmatrix} \quad (5)$$

Therefore, the component of the magnetic field with M_0 in the Z-direction will be related to the component of the magnetic field with M_0 in Y-direction as: $H_x=H_X$, $H_y=H_Z$, $H_z=-H_Y$. Similarly, the coordinates x, y, and z as well as the bar-magnet dimensions, x_b, y_b, and z_b, are to be transformed in the same way as: x=X, y=Z, and z=-Y and $x_a=X_a$, $y_a=Z_a$, and $z_a=-Y_a$. Using these transformations, the expressions for the magnetic H-field components with M_0 in the positive Z-direction are as follows:

$$H_X(X,Y,Z)=\frac{M_0}{4\pi}\sum_{k,l,m=1}^{2}(-1)^{k+l+m}$$
$$\ln\left\{-(Y+(-1)^l(-Y_b))+\sqrt{\left[X+(-1)^k X_b\right]^2+\left[-(Y+(-1)^l(-Y_b))\right]^2+\left[Z+(-1)^m Z_b\right]^2}\right\} \quad (6)$$

$$H_Y(X,Y,Z)=\frac{-M_0}{4\pi}\sum_{k,l,m=1}^{2}(-1)^{k+l+m}$$
$$\ln\left\{X+(-1)^k X_b+\sqrt{\left[X+(-1)^k X_b\right]^2+\left[-(Y+(-1)^l(-Y_b))\right]^2+\left[Z+(-1)^m Z_b\right]^2}\right\} \quad (7)$$

$$H_Z(X,Y,Z)=\frac{-M_0}{4\pi}\sum_{k,l,m=1}^{2}(-1)^{k+l+m}\frac{\left[Z+(-1)^m Z_b\right]\left[X+(-1)^k X_b\right]}{\left|Z+(-1)^m Z_b\right|\left|X+(-1)^k X_b\right|}$$
$$\times\arctan\left\{\frac{\left|X+(-1)^k X_b\right|\cdot\left[-(Y+(-1)^l(-Y_b))\right]}{\left|Z+(-1)^m Z_b\right|\cdot\sqrt{\left[X+(-1)^k X_b\right]^2+\left[-(Y+(-1)^l(-Y_b))\right]^2+\left[Z+(-1)^m Z_b\right]^2}}\right\} \quad (8)$$

Using the relation $B=\mu_0 H$, the B-field components can be calculated at any point (X,Y,Z) outside of the bar-magnet. Figure 6 shows a plot of B-field in the Z-direction as a function of Z for different values of M_0.

It can be seen that the slope of the curves changes with different values of the magnetization parameter, M_0. We note that, as experimentally expected, the H_x (X, Y,Z) and H_y(X,Y,Z) are zero for X=0, Y=0, and for any Z.

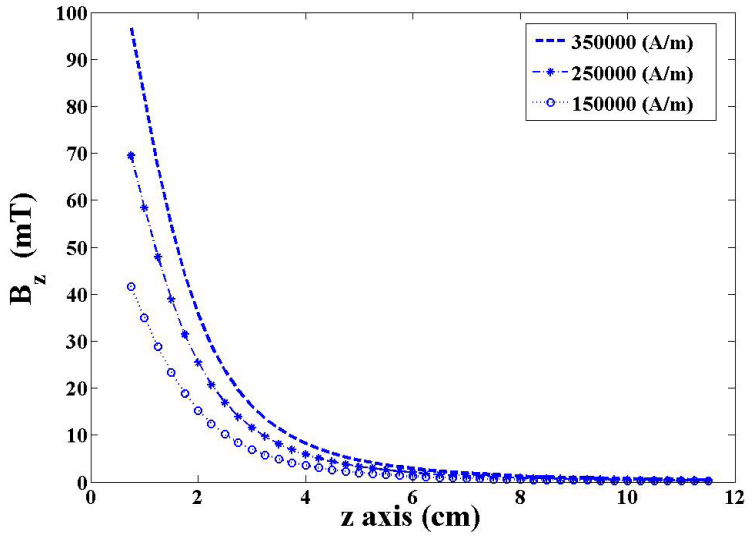

Figure 6. Plots of B_Z versus Z for different values of the magnetizations parameter (M_0) given X=0 and Y=0.

3. Results

3.1. Determination of M_0

In this research, we measured the magnetic flux density, B, of the bar-magnet along the magnetization direction Z. Since the B_Z field in Z direction depends only on the M_0, the bar magnet dimensions, and on the distance Z, therefore, for the known values of X_b, Y_b, and Z_b, the B_Z can be plotted as a function of Z together with the experimental data as shown in Figure 7. The parameter M_0 in the formula can then be adjusted to bring the analytical curve overlapping the experimental data. For the experimental data shown in Figure 7, The M_0 is found to be 280000 A/m.

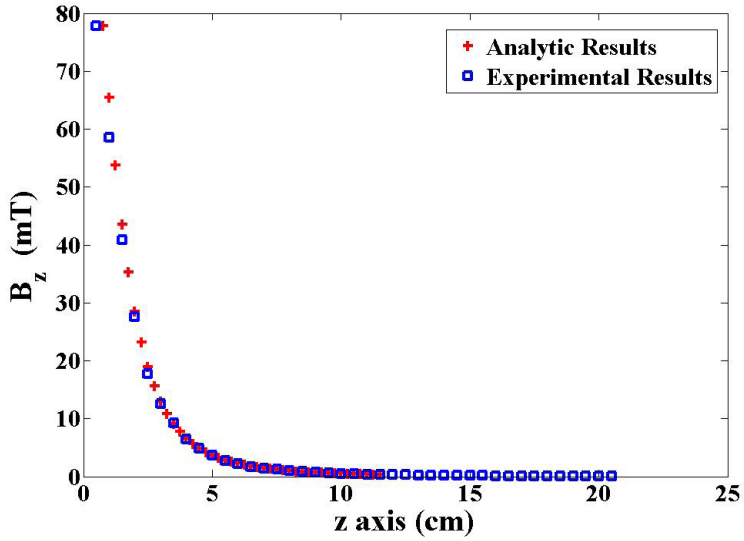

Figure 7. Analytical fitting of the B_Z field curve on the experimental data with M_0=280000 A/m.

4. Discussion

First of all, the accuracy of MFMIM as a device for measuring the magnetic flux intensity and the magnetic field magnitude and its functions has been investigated in this paper. In addition, we benchmarked our results with commercial grades experimentally to be ensured enough that our results are acceptable and accurate for calculating the magnetization parameter. In this article, we also presented a new method for determining the magnetization parameter of a bar-shaped permanent magnet. In this method, assuming that the bar-magnet is only magnetized in the z direction, we have used the analytical expression for the magnetic H-field in the Z-direction to find this parameter. The magnetization parameter has been determined by fitting the analytical curve to the experimental data in the Z-direction by adjusting the M_0 parameter. The fitting parameter, M_0, in this investigation is found to be 280000 A/m which is in the range of acceptable values for a bar magnet. This also is a proof of accuracy of our device's result in other applications such as the measurement of magnetic field magnitude in most of the MRI modulus.

References

1- M. Kabir, H. Mashayekhi, S. Aftabi, Magnetic Field Magnitude and Intensity Meter in Non-Solid Environment Using Magnetic Permeability Constant, Iranian Industrial Property General and Patent Office, Patent No. 83637, 2014.

2- C. F. Gauss, The Intensity of the Earth's Magnetic Force Reduced to Absolute Measurement. Library of Congress, class QC827, book G27, 1995.

3- J. Jankowski, C. Sucksdorff, IAGA Guide for Magnetic Measurements and Observatory Practice. International Association of Geomagnetism and Aeronomy, Poland, Warsaw, ISBN 0-9650686-2-5, 1996.

4- J. E. Lenz, A review of magnetic sensors. Proc. of IEEE, 78(6): 973–989, 1990.

5- J. L. Salpeter, Permanent Magnets. Journal of the British Institution of Radio Engineers; 98(2557):211-249, 1948.

6- W. D. Callister, Jr. and D. G. Rethwisch, Materials science and engineering, an introduction. John Wiley & Sons; 8th edition, 2010.

7- J. R. Reitz, F. J. Milford, R. W. Christy, Foundation of Electromagnetic Theory. Addison-Wesley; 4th edition, 1993.

8- E. W. Collings, M. D. Sumption, and E. Lee, Magnetization as a Critical Defining Parameter for Strand in Precision Dipole Applications -Implications for Field Error and F-J Stability. IEEE Transactions on Applied Superconductivity; 2(1): 308-318, 2001.

9- J. F. Gieras and M. Wing, Permanent Magnet Motor Technology: Design and Applications. Marcel Dekker; 2nd edition, 2002.

10- M. M. Tomiak, J. D. Rosenblum, J. M. Prager and C. E. Metz, Magnetization Transfer: A Potential Method to Determine the Age of Multiple Sclerosis Lesions. American Journal of Neuroradiology; 15(1):1569-1574, 1994.

11- R. C. Mehta, G. B. Pike and D. R. Enzmann, Magnetization transfer magnetic resonance imaging: a clinical review. Topics in Magnetic Resonance Imaging; 8(1): 214-30, 1996.

12- K. Fabian, some additional parameters to estimate domain state from isothermal magnetization measurements. Earth and Planetary Science Letters; 213(1): 337-345, 2003.

13- www.hengtonggroup.com/en/.

14- R. Engel-Herbert and T. Hesjedal, Calculation of the magnetic stray field of a uniaxial magnetic domain. Journal of Applied Physics; 97(1): 504-507, 2005.

15- G. B. Arfken and H. J. Webber, Mathematical Methods for Physicists. New York: Academic Press; 1995.